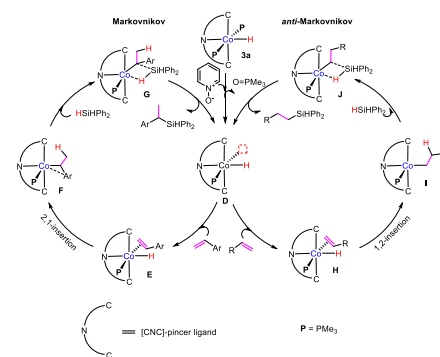


# [CNC]-Pincer Cobalt Hydride Catalyzed Distinct Selective Hydrosilylation of Aryl Alkene and Alkyl Alkene

Shangqing Xie, Xiaoyan Li,\* Hongjian Sun,\* Olaf Fuhr, and Dieter Fenske

**ABSTRACT:** The reactions of unsymmetrical N heterocyclic carbene (NHC) [CNC] pincer preligands with  $\text{CoMe}(\text{PMe}_3)_4$  gave rise to NHC [CNC] pincer cobalt(III) hydrides,  $[(\text{C}_{\text{carbene}}\text{N}_{\text{amino}}\text{C}_{\text{naphthyl}})\text{Co}(\text{H})(\text{PMe}_3)_2]$  (**3a**) and (**3b**), via  $\text{C}_{\text{sp}^2}\text{-H}$  activation and the unexpected *trans* bischelate  $[\text{C}_{\text{carbene}}\text{N}_{\text{amino}}]$  cobalt(II) complexes **4a** and **4b** via a disproportionation reaction, respectively. It was found that both **3a** and **3b** are efficient catalysts for hydrosilylation of alkenes. With aryl alkenes as substrates, **3a** has high Markovnikov selectivity in excellent yields, while **3a** is an efficient *anti* Markovnikov catalyst in good yields with alkyl alkenes as substrates. The catalytic process could be promoted with pyridine N oxide as an initiator. The catalytic mechanisms for the two different selectivities were proposed. Complexes **3a**, **3b**, **4a**, and **4b** were characterized by spectroscopic methods, and the molecular structures of **3b**, **4a**, and **4b** were determined by single crystal X ray diffraction.



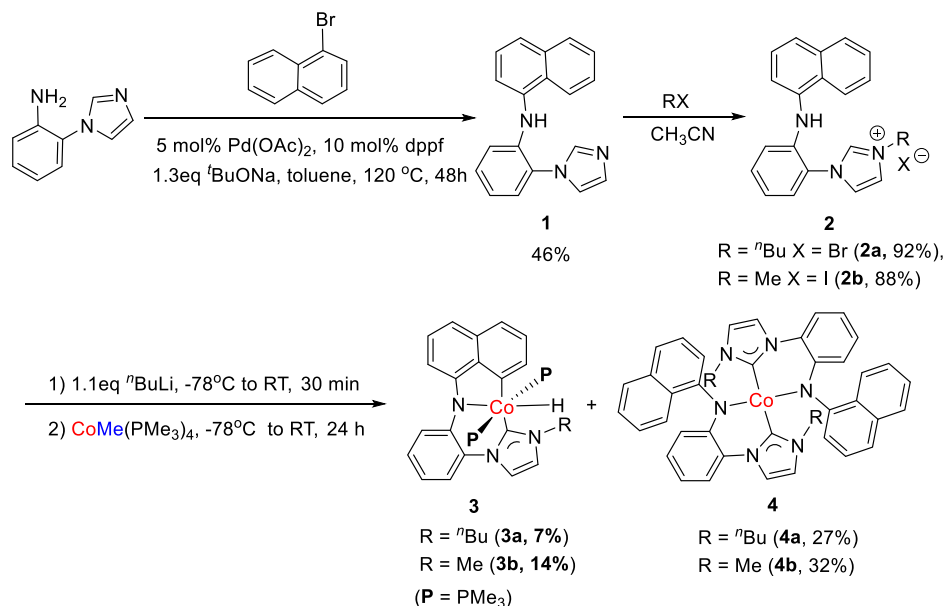
## 1. INTRODUCTION

Organosilicon compounds have been widely used in electronics, building materials, textiles, the light industry, medical treatments, transportation, and plastic rubber and other industries and gradually penetrated into people's daily lives.<sup>1,2</sup> Transition metal catalyzed hydrosilylation of alkenes is an important method for the synthesis of organosilicon compounds. At present, the catalysts successfully used in industrial production are platinum complexes.<sup>3</sup> However, platinum complexes as catalysts have some disadvantages. On the one hand, the platinum catalyst as a precious metal compound in the hydrosilylation of alkenes cannot be regenerated. On the other hand, the toxicity of residual platinum in the final silicon containing products to a certain extent limits the application of silicon materials. In recent years, with people's increasing attention to environmental protection and the pursuit of sustainable development, we gradually began to seek the replacement of precious metal catalysts in the field of catalytic chemistry. The environmental friendly base metal cobalt as the congeneric element of precious metals has attracted the attention of chemists. Since Chalk and Harrod found that  $\text{Co}_2(\text{CO})_8$  could catalyze the hydrosilylation of terminal alkenes with anti Markovnikov selectivity,<sup>4</sup> some cobalt complexes have been synthesized to catalyze the hydrosilylation of alkenes.<sup>5-14</sup> However, there are few reports on cobalt catalyzed hydrosilylation of alkenes with Markovnikov selectivity.<sup>14</sup> In 2016, Huang and co workers prepared a series of [PNN] pincer metal complexes to catalyze the hydrosilylation of alkenes and found the related iron complexes were selective for anti Markovnikov hydrosilylation, while the related cobalt complexes provided the

Markovnikov product in high yield.<sup>6</sup> In 2018, Deng and co workers disclosed that  $(\text{IMes})_2\text{CoCl}$  was an efficient catalyst for the hydrosilylation of alkenes. When aryl substituted alkenes were employed as substrates,  $(\text{IMes})_2\text{CoCl}$  generated the Markovnikov hydrosilylation products in most cases. Meanwhile, the *anti* Markovnikov hydrosilylation products could be obtained when aliphatic alkenes were studied as substrates.<sup>7</sup> The case of the substrate dependent regioselectivity can also be found in Trovitch's work, and the difference of the stability of the alkyl cobalt intermediates generated in the reaction may be responsible for different selectivities.<sup>27</sup> Unlike Deng's and Huang's work, Lu and co workers reported a cobalt catalyst for alkene hydrosilylation in 2017. This catalytic system afforded the same regioselectivity for styrenes and aliphatic alkenes using the same cobalt catalyst and showed stronger selectivity.<sup>14</sup> In addition, in the transition metal mediated hydrosilylation of alkenes, metal hydride is considered a key intermediate,<sup>15</sup> but there are rare examples to study the hydrosilylation of alkenes with metal hydride as a catalyst.

In this paper, two [CNC] pincer cobalt(III) hydrides were synthesized. It was found that the cobalt hydrides as catalysts are highly selective for Markovnikov hydrosilylation of aryl alkenes and for *anti* Markovnikov hydrosilylation of alkyl

## Scheme 1. Synthesis of [CNC] Pincer Cobalt Hydrides **3a** and **3b**



alkenes. The catalytic process could be promoted with pyridine N oxide as an initiator. The proposed mechanisms of the catalytic hydrosilylation of alkenes were discussed and partially experimentally verified. The key step in the catalytic cycle is the insertion of alkene into the Co–H bond. For this hydrosilylation reaction, the alkyl cobalt(III) intermediate was proposed as the key intermediate.

## 2. RESULTS AND DISCUSSION

### 2.1. Synthesis of [CNC]-Cobalt Hydrides **3**.

The unsymmetrical N heterocyclic carbene (NHC) ligand precursors **2**, imidazolium salts, were synthesized according to the reported method (Scheme 1).<sup>16</sup> After the lithiation of **2** with <sup>n</sup>BuLi, CoMe(PMe<sub>3</sub>)<sub>4</sub> was added to give rise to a mixture of the expected [CNC] pincer cobalt hydride **3** and unexpected *trans* bischelate cobalt(II) complex **4**. The extraction of the crude mixture with *n* pentane and recrystallization from the concentrated *n* pentane solution afforded yellow crystals of **3a** and **3b**. After that, the extraction of the residue with diethyl ether and recrystallization from the concentrated diethyl ether solution provided orange crystals of **4a** and **4b**.

Complexes **3** and **4** are sensitive to moisture and air. In the infrared spectra of complexes **3a** and **3b**, the typical  $\nu(\text{Co}-\text{H})$  stretching vibrations were found at 1904 cm<sup>-1</sup> (**3a**) and 1920 cm<sup>-1</sup> (**3b**), respectively. The NMR analyses of complexes **3a** and **3b** are consistent with their compositions. In the <sup>1</sup>H NMR spectra, the hydrido signal was shifted significantly upfield to -21.21 ppm (**3a**) and -22.14 ppm (**3b**), respectively. The signal split into a triplet peak, owing to the coupling with the coordinated P atoms (<sup>2</sup>J<sub>H,P</sub> = 69 Hz). The <sup>31</sup>P NMR resonances of complexes **3a** and **3b** appeared at 17.18 and 17.82 ppm as a singlet, respectively, suggesting the presence of two equivalent PMe<sub>3</sub> ligands.

The solid state molecular structure of complex **3b** was confirmed by single crystal X ray diffraction analysis (Figure 1). The central cobalt atom of complex **3b** is situated in a distorted octahedral geometry surrounded by a *mer* [CNC] pincer ligand and two PMe<sub>3</sub> ligands disposed *trans* to each other (P1–Co1–P2 = 167.08°) as well as a hydrido ligand. In

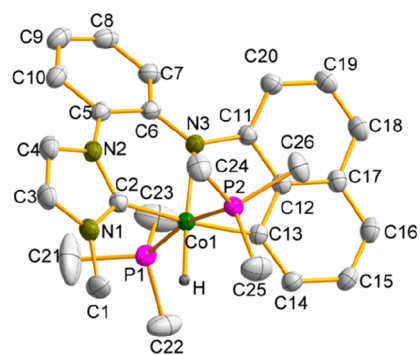


**Figure 1.** Molecular structure of **3b** at the 50% probability level. Hydrogen atoms except for the hydrido atom are omitted for clarity. Selected bond lengths (Å) and angles (deg): Co1–H1 1.34(4), Co1–P1 2.165(4), Co1–P2 2.208(4), Co1–N3 2.001(11), Co1–C2 1.906(13), Co1–C13 1.941(13); P1–Co1–P2 167.081(16), N3–Co1–P1 96.11(3), N3–Co1–P2 95.41(3), C2–Co1–P1 94.82(4), C2–Co1–P2 90.69(4), C2–Co1–N3 91.62(5), C2–Co1–C13 174.09(5), C13–Co1–P1 90.06(4), C13–Co1–P2 85.22(4), C13–Co1–N3 84.53(5), P1–Co1–H1 82.3(15), P2–Co1–H1 85.6(15), N3–Co1–H1 172.9(15), C2–Co1–H1 95.4(15), C13–Co1–H1 88.6(15).

complex **3b**, the Co–C<sub>(carbene)</sub> distance (Co1–C2 = 1.906(13) Å) is shorter than the Co<sub>1</sub>–C<sub>13</sub> distance (1.941(13) Å) due to the double bond component in the Co–C<sub>(carbene)</sub> bond and is in the range of those of other NHC cobalt complexes.<sup>17</sup> The Co<sub>1</sub>–H<sub>1</sub> bond length (1.34(4) Å) is slightly shorter than the normal bond length of Co–H bonds (1.40–1.50 Å).<sup>18</sup>

Complexes **4a** and **4b** are different from the other bischelate NHCs metal complexes.<sup>19</sup> Paramagnetic complexes **4a** and **4b** are soluble in diethyl ether and insoluble in *n* pentane. The molecular structures of **4a** and **4b** were also confirmed by single crystal X ray diffraction analysis (Figures 2 and 3). The structures of **4a** and **4b** feature a distorted tetrahedral Co(II) center with two *trans* positioned [C,N] chelate ligands bearing the naphthalene rings. The averaged Co–C<sub>NHC</sub> and Co–N<sub>amino</sub> bond lengths are 1.998(5) and 1.971(3) Å, respectively, close to those of the analogous complexes.<sup>20</sup>

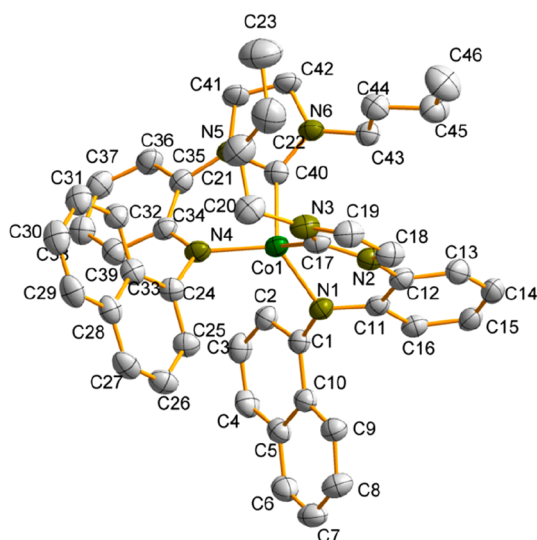


**Figure 2.** Molecular structure of **4a** at the 50% probability level. Hydrogen atoms are omitted for clarity. Selected bond lengths (Å) and angles (deg): Co1–N1 1.971(3), Co1–N4 1.940(4), Co1–C1 1.997(5), Co1–C2 1.998(5); N1–Co1–C17 91.78(16), N1–Co1–C40 124.52(16), N4–Co1–N1 119.76(15), N4–Co1–C17 120.06(17), N4–Co1–C40 92.98(16), C17–Co1–C40 109.85(18).

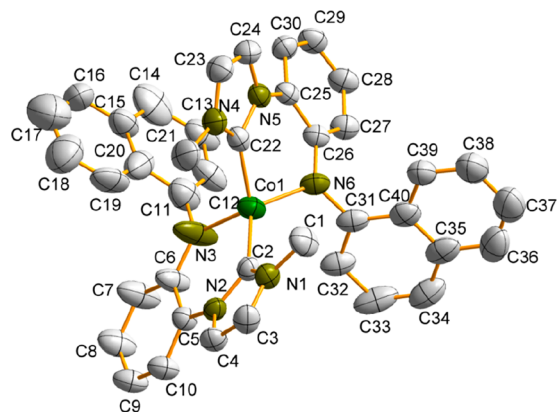


**Figure 3.** Molecular structure of **4b** at the 50% probability level. Hydrogen atoms are omitted for clarity. Selected bond lengths (Å) and angles (deg): Co1–N3 1.909(5), Co1–N6 1.944(4), Co1–C1 1.987(5), Co1–C2 1.990(5); N3–Co1–N6 121.7(3), N3–Co1–C2 91.8(2), N3–Co1–C22 114.1(2), N6–Co1–C2 122.81(18), N6–Co1–C22 91.47(17), C2–Co1–C22 117.15(19).

The formation mechanisms of **3** and **4** are proposed in [Scheme 2](#). At first, the imidazolium halide salt reacts with <sup>t</sup>BuLi to afford NHC ligand **A**. We deduce that the reaction of **A** with CoMe(PMe<sub>3</sub>)<sub>4</sub> affords intermediate **B** via N–H bond activation and, in this process, cobalt(I) is oxidized to cobalt(III) center. Intermediate **C** is formed from **B** through reductive elimination with the release of a methane molecule. Complex **3**, a cobalt(III) hydride, is formed by the C<sub>sp<sup>2</sup></sub>–H bond activation of the naphthyl group. However, the disproportionation of two molecules of **C** delivers stable *trans* bischelate cobalt(II) complex **4** in higher yields with Co(PMe)<sub>4</sub> as a byproduct. Co(PMe)<sub>4</sub> can be proved by an IR spectrum of the mother solution.

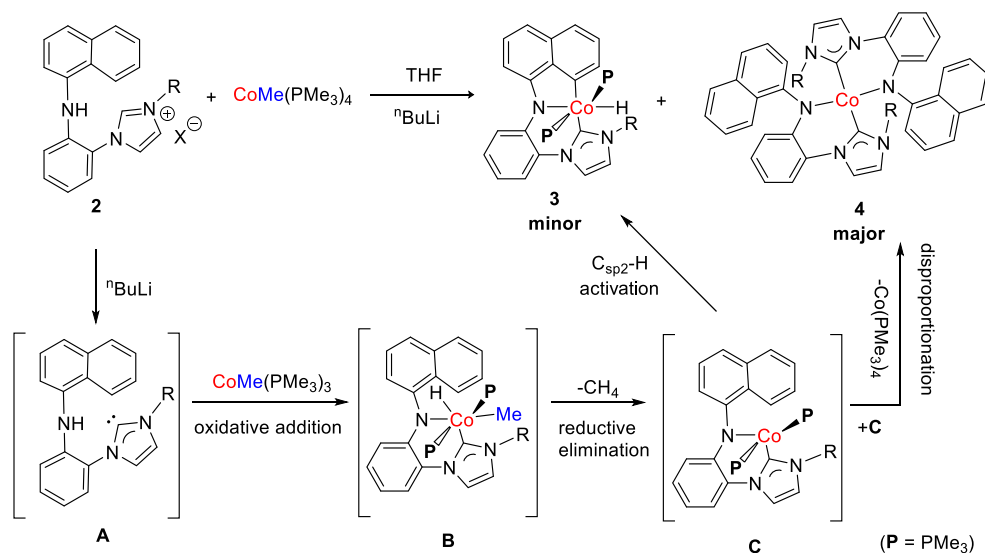
**2.2. Hydrosilylation of Alkenes with [CNC]-Pincer Cobalt(III) Hydrides **3** as Catalysts.** With **3** as catalysts, we initially evaluated their catalytic activity for the hydrosilylation

of styrene with Ph<sub>2</sub>SiH<sub>2</sub> at 70 °C for 10 h ([Scheme 3](#)). The experimental results are summarized in [Table 1](#). From [Table 1](#), we know that the reaction has a conversion of 98% in excellent selectivity (b/l = 94:6) with **3a** as a catalyst without solvent (entry 1, [Table 1](#)). The reaction selectivity in common solvents is not as good as that in solvent free reactions (entries 1 and 2–6, [Table 1](#)). Complex **3a** has a little bit better catalytic activity and selectivity than complex **3b** (entries 1 and 7, [Table 1](#)). When the reaction temperature dropped from 70 to 50 °C and 25 °C, the conversion decreased from 90% to 87% and 56%, respectively, but the selectivity is still good (entries 1 and 8–9, [Table 1](#)). If the catalyst loading decreased from 1 mol % to 0.5% and 0.1%, the conversion decreased from 98% to 91% and 69%, respectively (entries 1 and 10–11, [Table 1](#)). When the reaction time was shortened to 6 h, the conversion was reduced to 83% (entry 12, [Table 1](#)). A longer reaction time (12 h) resulted in only a slight increase in conversion (entry 13, [Table 1](#)). In addition, when various silanes were used for the reaction, Ph<sub>2</sub>SiH<sub>2</sub> had the best catalytic result (entries 1 and 14–18, [Table 1](#)). It was also found that the addition of pyridine N oxide at 25 °C increased the conversion from 78% to 95% within 24 h (entries 19–20) and with better selectivity (b/l = 96:4). This suggests that pyridine N oxide can significantly promote the reaction. It is considered that the addition of pyridine N oxide facilitates the dissociation of PMe<sub>3</sub> ligand of complex **3** by the formation of stable O=PMe<sub>3</sub>. This result indicates that the formation of an active unsaturated coordination intermediate produced via dissociation of PMe<sub>3</sub> is the first step in the catalytic cycle. The vacant coordination site is essential for the coordination of styrene with the cobalt center. Therefore, the optimized reaction conditions are as follows: 1 mol % **3a**, Ph<sub>2</sub>SiH<sub>2</sub>, solvent free, 25 °C, 24 h, and pyridine N oxide.

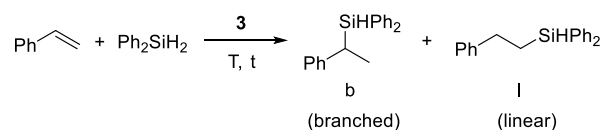
Under the optimized conditions, we explored the substrate scope of alkenes with [CNC] pincer cobalt hydride **3a** as a catalyst ([Table 2](#)). High Markovnikov regioselectivities were observed in the hydrosilylation of the aryl alkenes bearing halogen (**5e–5f**), methoxy (**5i**), methyl (**5b–5d**), *tert* butyl (**5h**), trifluoromethyl (**5k** and **5l**), and phenyl (**5m**) groups. The synthesis of **5e** was only mentioned in one patent while there are a few reports on the synthesis of the other reaction products.<sup>21</sup> The results in [Table 2](#) indicate that the electronic properties of the aryl group have a significant effect on the selectivity of the hydrosilylation of the alkenes. The aryl alkenes with the electron withdrawing substituents gave a lower selectivity compared to the aryl alkenes with the electron donating substituents. The steric hindrance of the substituents has little influence upon the catalytic reaction compared to the electronic property of the substrate. As the phenyl alkenes, the naphthyl alkenes could also undergo hydrosilylation to afford the corresponding product in modest to good yields with high regioselectivities (**5n** and **5o**). For the diphenyl substituted alkene, 1,1 diphenyl ethylene, the cobalt complex **3a** had no catalytic activity due to the strong steric effect of the two phenyl groups (**5p**). Surprisingly, alkyl alkenes exhibited reverse regioselectivity to aryl alkenes toward *anti* Markovnikov addition (**5q–5t**). This indicates that the aromatic rings in the aryl alkenes might play an important role for Markovnikov selectivity. In this catalytic system, allyl benzene also afforded an *anti* Markovnikov addition product (**5r**) with excellent selectivity.

**2.3. Mechanistic Study.** The reaction mechanisms of the hydrosilylation of alkenes catalyzed by metal complexes have

## Scheme 2. Suggested Formation Mechanisms of 3 and 4



## Scheme 3. Template Reaction



been extensively studied in recent years.<sup>22,23</sup> Usually, these reaction mechanisms can be divided into two types, the Chalk–Harrod mechanism and the modified Chalk–Harrod mechanism. They have different intermediates.<sup>24,25</sup>

In order to better understand the mechanism of the catalytic reaction, we studied the effect of the addition sequence of the reactants (Table S3). The experiments show that we could get the same results as in Table 1 if the catalyst 3a reacted with

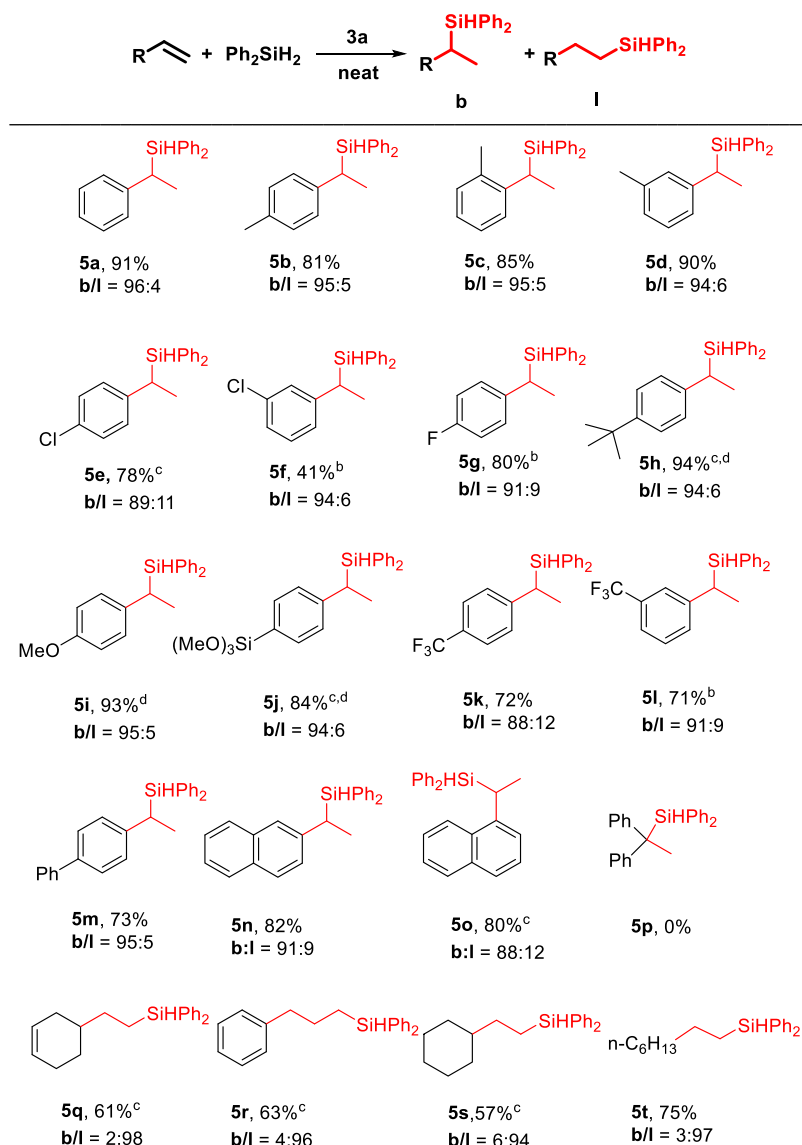
styrene for 30 min before adding Ph<sub>2</sub>SiH<sub>2</sub>. If the catalyst 3a reacted with Ph<sub>2</sub>SiH<sub>2</sub> for 30 min before adding styrene, the conversion was reduced from 98% to 55%, and the selectivity was also greatly decreased from 94:6 to 72:28. This experiment implies that precatalyst 3a can react with silane to give another complex having a detrimental effect and also indicates that the reaction of 3a with the alkene is the first step in the catalytic cycle. The stoichiometric reactions between 3a and styrene as well as between 3a and Ph<sub>2</sub>SiH<sub>2</sub> were carried out. Unfortunately, all attempts to isolate the intermediates failed. However, some experiments provide important information to the mechanism. The reaction of 4 *tert* butylstyrene (10 equiv) with 3a (1 equiv) was monitored by *in situ* NMR. As the reaction progressed, both the hydrido resonance (−22.22 ppm) of 3a in the <sup>1</sup>H NMR spectra and the phosphorus signal

**Table 1. Optimization of Reaction Conditions<sup>a</sup>**

entry	catalyst	loading (mol %)	solvent	silane	temp (°C)	time (h)	conv. (%)	ratio (b/l) <sup>b</sup>
1	3a	1	neat	Ph <sub>2</sub> SiH <sub>2</sub>	70	10	98	94:6
2	3a	1	THF	Ph <sub>2</sub> SiH <sub>2</sub>	70	10	64	65:35
3	3a	1	toluene	Ph <sub>2</sub> SiH <sub>2</sub>	70	10	93	85:15
4	3a	1	dioxane	Ph <sub>2</sub> SiH <sub>2</sub>	70	10	89	70:30
5	3a	1	DME	Ph <sub>2</sub> SiH <sub>2</sub>	70	10	67	56:44
6	3a	1	MeCN	Ph <sub>2</sub> SiH <sub>2</sub>	70	10	29	69:31
7	3b	1	neat	Ph <sub>2</sub> SiH <sub>2</sub>	70	10	97	92:8
8	3a	1	neat	Ph <sub>2</sub> SiH <sub>2</sub>	50	10	87	95:5
9	3a	1	neat	Ph <sub>2</sub> SiH <sub>2</sub>	25	10	56	95:5
10	3a	0.5	neat	Ph <sub>2</sub> SiH <sub>2</sub>	70	10	91	93:7
11	3a	0.1	neat	Ph <sub>2</sub> SiH <sub>2</sub>	70	10	69	93:7
12	3a	1	neat	Ph <sub>2</sub> SiH <sub>2</sub>	70	6	83	94:6
13	3a	1	neat	Ph <sub>2</sub> SiH <sub>2</sub>	50	12	99	94:6
14	3a	1	neat	PhSiH <sub>3</sub>	70	10	0	
15	3a	1	neat	Ph <sub>3</sub> SiH	70	10	53	
16	3a	1	neat	(EtO) <sub>3</sub> SiH	70	10	45	
17	3a	1	neat	Et <sub>3</sub> SiH	70	10	18	
18	3a	1	neat	(EtO) <sub>2</sub> SiHMe	70	10	35	
19	3a	1	neat	Ph <sub>2</sub> SiH <sub>2</sub>	25	24	78	95:5
20 <sup>c</sup>	3a	1	neat	Ph <sub>2</sub> SiH <sub>2</sub>	25	24	95	96:4

<sup>a</sup>Catalytic reaction conditions: styrene (1.0 mmol), silane (1.2 mmol), solvent (1 mL), conversions and product ratios were determined by GC with *n* dodecane as an internal standard. <sup>b</sup>b/l: branched/linear. <sup>c</sup>With pyridine N oxide (1.0 mmol).

Table 2. Scope of Alkenes for Cocatalyzed Hydrosilylation<sup>a</sup>



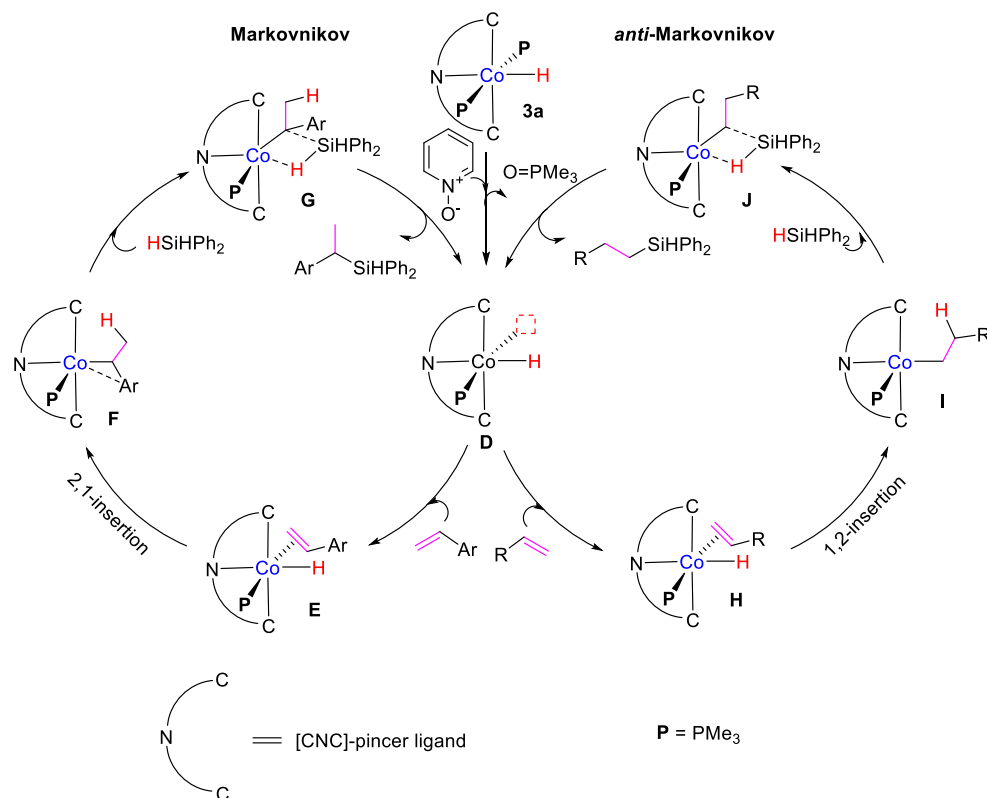
<sup>a</sup>Catalytic reaction conditions: alkene (1.0 mmol), Ph<sub>2</sub>SiH<sub>2</sub> (1.2 mmol), pyridine N oxides (1 mol %), and 3a (1 mol %) were stirred in neat conditions at 25 °C for 24 h. Product ratios and yields were determined by GC with *n* dodecane as the internal standard. <sup>b</sup>5 mol % 3a was provided. <sup>c</sup>Alkene (1.0 mmol), Ph<sub>2</sub>SiH<sub>2</sub> (1.2 mmol), and 3a (1 mol %) were stirred in neat conditions at 70 °C for 12 h without additive. <sup>d</sup>Isolated yields.

(17.18 ppm) of 3a in the <sup>31</sup>P NMR spectra gradually disappeared. At the same time, an increasingly strong phosphorus signal at 30.79 ppm appeared (Figures S1 and S2). We speculate that the signal at 30.79 ppm in the <sup>31</sup>P NMR spectra might belong to intermediate F or I, the alkyl cobalt intermediate in Scheme 4. Additionally, a trace amount of byproduct 3 octene could be detected from the reaction of 1 octene with Ph<sub>2</sub>SiH<sub>2</sub> (Figure S3). This alkene isomerization is attributed to the β H elimination after the insertion of the C=C bond into the Co-H bond.<sup>26</sup>

Despite some experimental attempts to prove the mechanism, there is still no way to truly exclude the possibility of other mechanisms. On the basis of the current experimental results and literature reports, we propose a possible catalytic cycle for hydrosilylation of alkene catalyzed by cobalt hydride (Scheme 4).<sup>27–29</sup> At the beginning of the reaction, the introduction of pyridine N oxide accelerates the dissociation of

the PMe<sub>3</sub> ligand and provides intermediate D with an empty coordinate site, which can be occupied by alkene to form E or H. The insertion of alkene into the Co-H bond occurs subsequently to afford intermediate F or I, an alkyl cobalt intermediate. This is considered as an important foundation for the hydrofunctionalization of alkenes.<sup>24</sup> It is noteworthy that the structures of F and I are also speculative, and the present experimental results cannot confirm their structures. This step determines the regioselectivity of the reaction. For aryl alkenes, the migration insertion is more biased toward the 2,1 insertion to form a thermodynamically preferred secondary benzyl cobalt species F. In addition, the π-π interaction between the phenyl of aryl alkene and naphthalene ring of the catalyst and the weak coordination effect between the cobalt and phenyl of aryl alkene may be also responsible for the 2,1 insertion mode.<sup>30</sup> Contrary to aryl alkene, alkyl alkene is more suitable for 1,2 insertion to generate a primary alkyl cobalt

## Scheme 4. Proposed Mechanisms



species **I** because intermediate **I** is more reactive to  $\sigma$  bond metathesis.<sup>24</sup>  $\text{H}_2\text{SiPh}_2$  coordinates to the Co center in **F** or **I** to form a four membered ring transition state **G** or **J**. The final silane product is generated through  $\sigma$  bond metathesis with the regeneration of real catalyst **D**. For this hydrosilylation reaction, alkyl cobalt(III) intermediate **F** or **I** is proposed as the key intermediate. This is different from the mechanisms proposed by the groups of Huang and Deng.<sup>6,7</sup> They consider that silyl metal complexes are the key intermediates of the reactions.

### 3. CONCLUSION

Two novel NHC [CNC] pincer cobalt(III) hydrides **3a** and **3b** were obtained from the reactions of preligands with  $\text{CoMe}(\text{PMe}_3)_4$ . It was found that **3a** is an efficient catalyst for the hydrosilylation of alkenes. The experimental results indicate that Markovnikov products were formed with aryl alkenes as substrates while *anti* Markovnikov silanes could be produced with alkyl alkenes as substrates. The addition of pyridine N oxide promoted the catalytic process significantly. The catalytic conditions are milder with excellent regioselectivity compared with the results from the literature.<sup>7</sup> This catalytic system is tolerant of a broad range of the substrates with different substituents in moderate to good yields. The catalytic mechanisms are proposed on the basis of the experimental information and literature reports. For this possible hydrosilylation mechanism, the alkyl cobalt(III) intermediate is proposed as the key intermediate.

### 4. EXPERIMENTAL SECTION

**4.1. General Procedures.** All experiments and manipulations were carried out under nitrogen atmosphere using standard Schlenk techniques, unless otherwise noted. All solvents were dried by general

methods and freshly distilled before use.  $\text{CoMe}(\text{PMe}_3)_4$  was prepared according to the reported procedure.<sup>31</sup> The other chemicals were purchased from commercial sources and used as received. Infrared spectra ( $4000\text{--}400\text{ cm}^{-1}$ ) were recorded on a Bruker ALPHA FT IR instrument by using Nujol mulls between KBr disks. The  $^1\text{H}$ ,  $^{13}\text{C}$ , and  $^{31}\text{P}$  NMR spectra were recorded with a Bruker 300 spectrometer. Elemental analyses were carried out on an Elementar Vario ELIII instrument. Gas chromatography was performed with *n* dodecane as an internal standard.

**4.2. Synthesis of 1.** A Schlenk flask was charged with 2 (1*H* imidazol 1 yl)aniline (0.79 g, 5 mmol), 1 bromonaphthalene (1.035 g, 5 mmol),  $\text{Pd}(\text{OAc})_2$  (0.05612 g, 0.25 mmol), 1,1' bis (diphenylphosphino) ferrocene (dppf) (0.2772 g, 0.5 mmol),  $^t\text{BuONa}$  (0.624 g, 6.5 mmol), and toluene (30 mL) under a nitrogen atmosphere. The reaction mixture was then heated for 48 h at  $110\text{ }^\circ\text{C}$ . After cooling to room temperature, the precipitate was filtered and washed with  $\text{CH}_2\text{Cl}_2$ . The combined organic fractions were then evaporated under vacuum, and the crude product was purified by column chromatography on silica gel (dichloromethane/methanol (200:1)) to obtain an orange solid. Yield: 0.65 g, 46%. Mp:  $150.9\text{--}152.2\text{ }^\circ\text{C}$ .  $^1\text{H}$  NMR (300 MHz,  $\text{CDCl}_3$ , 298 K, ppm): 5.61 (s, 1H, N-H), 6.83–7.80 (m, 14H, Ar-H).  $^{13}\text{C}$  NMR (75 MHz,  $\text{CDCl}_3$ , 298 K, ppm): 115.3, 118.2, 118.6, 120.9, 123.9, 124.8, 125.1, 125.3, 126.2, 127.7, 128.7, 133.6, 135.7, 140.1 (NCN).

**4.3. Synthesis of 2a.** To a solution of **1** (1.29 g, 5 mmol) in acetonitrile (50 mL) was added *n*  $\text{C}_4\text{H}_9\text{Br}$  (1.37 g, 10 mmol). The reaction mixture was refluxed for 24 h. After cooling to room temperature, the precipitate was filtered and washed with  $\text{CH}_3\text{OH}$  (20 mL). The combined organic fractions were then evaporated under vacuum, and the crude product was recrystallized from  $\text{CH}_3\text{OH}/\text{Et}_2\text{O}$  to give **2a** (1.94 g) as an orange solid in 92% yield. Mp:  $197.7\text{--}198.5\text{ }^\circ\text{C}$ . Calcd for  $\text{C}_{23}\text{H}_{24}\text{BrN}_3$  (422.37 g/mol): C, 65.41; H, 5.73; N, 9.95. Found: C, 65.17; H, 5.40; N, 9.75.  $^1\text{H}$  NMR (300 MHz,  $\text{CDCl}_3$ , 298 K, ppm): 0.69–0.73 (t,  $J = 6\text{ Hz}$ , 3H,  $\text{CH}_3$ ), 0.96–1.09 (m, 2H,  $\text{CH}_2$ ), 1.45–1.55 (m, 2H,  $\text{CH}_2$ ), 4.00–4.05 (t,  $J = 15\text{ Hz}$ , 2H,  $\text{CH}_2$ ), 6.88–8.10 (m, 14H,  $H_{\text{arom}}$ ), 9.71 (s, 1H, NH).  $^{13}\text{C}$  NMR (75 MHz,  $\text{CDCl}_3$ , 298 K, ppm): 13.4 ( $C_{\text{aliphatic}}$ ), 19.4 ( $C_{\text{aliphatic}}$ ),

31.4 ( $C_{\text{aliphatic}}$ ), 50.0 ( $C_{\text{aliphatic}}$ ), 116.9 ( $C_{\text{aromatic}}$ ), 122.0 ( $C_{\text{aromatic}}$ ), 122.7 ( $C_{\text{aromatic}}$ ), 123.4 ( $C_{\text{aromatic}}$ ), 125.8 ( $C_{\text{aromatic}}$ ), 126.1 ( $C_{\text{aromatic}}$ ), 126.4 ( $C_{\text{aromatic}}$ ), 127.3 ( $C_{\text{aromatic}}$ ), 127.4 ( $C_{\text{aromatic}}$ ), 128.3 ( $C_{\text{aromatic}}$ ), 129.9 ( $C_{\text{aromatic}}$ ), 131.5 ( $C_{\text{aromatic}}$ ), 134.5 ( $C_{\text{aromatic}}$ ), 137.3 ( $C_{\text{aromatic}}$ ), 138.7 ( $C_{\text{aromatic}}$ ), 139.2 ( $C_{\text{aromatic}}$ ), 140.0 ( $C_{\text{aromatic}}$ ), 140.5 (NCN).

**4.4. Synthesis of 2b.** To a solution of **1** (1.29 g, 5 mmol) in acetonitrile (50 mL) was added MeI (1.41 g, 10 mmol). The reaction mixture was refluxed for 24 h. After cooling to room temperature, the precipitate was filtered and washed with  $\text{CH}_3\text{OH}$  (20 mL). The combined organic fractions were then evaporated under vacuum, and the crude product was recrystallized from  $\text{CH}_3\text{OH}/\text{Et}_2\text{O}$  to give **2b** (1.88 g) as a yellow solid in 88% yield. Mp: 200.4–201.0 °C. Calcd for  $\text{C}_{20}\text{H}_{18}\text{IN}_3$  (427.29 g/mol): C, 56.22; H, 4.25; N, 9.83. Found: C, 55.97; H, 4.17; N, 9.69.  $^1\text{H}$  NMR (300 MHz,  $\text{DMSO } d$ , 298 K, ppm): 3.81 (s, 3H,  $\text{CH}_3$ ), 6.62–6.85 (dd,  $J = 8.2$  Hz, 1.0 Hz, 1H,  $H_{\text{arom}}$ ), 7.04–7.09 (m, 2H,  $H_{\text{arom}}$ ), 7.35–7.44 (m, 2H,  $H_{\text{arom}}$ ), 7.50–7.55 (m, 3H,  $H_{\text{arom}}$ ), 7.66–7.69 (d,  $J = 9$  Hz, 1H,  $H_{\text{arom}}$ ), 7.77–7.78 (t,  $J = 3$  Hz,  $H_{\text{arom}}$ ), 7.92–8.09 (m, 4H,  $H_{\text{arom}}$ ), 9.56 (s, 1H, NH).  $^{13}\text{C}$  NMR (75 MHz,  $\text{DMSO } d$ , 298 K, ppm): 36.3 ( $C_{\text{aliphatic}}$ ), 118.7 ( $C_{\text{aromatic}}$ ), 119.8 ( $C_{\text{aromatic}}$ ), 120.9 ( $C_{\text{aromatic}}$ ), 124.1 ( $C_{\text{aromatic}}$ ), 124.3 ( $C_{\text{aromatic}}$ ), 126.2 ( $C_{\text{aromatic}}$ ), 126.5 ( $C_{\text{aromatic}}$ ), 126.7 ( $C_{\text{aromatic}}$ ), 128.7 ( $C_{\text{aromatic}}$ ), 131.8 ( $C_{\text{aromatic}}$ ), 134.6 ( $C_{\text{aromatic}}$ ), 138.3 ( $C_{\text{aromatic}}$ ), 138.6 ( $C_{\text{aromatic}}$ ), 141.6 (NCN).

**4.5. Synthesis of 3a and 4a.** A 0.63 mL sample of *n* BuLi (2.5 M in hexane, 1.58 mmol) was added slowly to 30 mL of a THF solution of ligand **2a** (0.6080 g, 1.44 mmol) at  $-78$  °C, and the solution turned red. When the temperature returned to room temperature, the mixture was stirred for 30 min. After that, a solution of  $\text{CoMe}(\text{PMe}_3)_4$  (0.5451 g, 1.44 mmol) in THF (30 mL) was added slowly to the resulting solution at  $-78$  °C. The reaction mixture was allowed to stir for 48 h at room temperature to provide a deep yellow solution. After the reaction, the solvents were removed under vacuum, and the residue was extracted with 100 mL of *n* pentane and 50 mL of diethyl ether, respectively. The dark orange crystals of **4a** were obtained at  $-10$  °C from the concentrated diethyl ether solutions. Yield: 289 mg, 27%. Mp: 189.8–190.3 °C. Calcd for  $\text{C}_{46}\text{H}_{44}\text{CoN}_6$  (739.83 g/mol): C, 74.68; H, 5.99; N, 11.36. Found: C, 74.77; H, 5.80; N, 11.55. The light yellow crystals of **3a** were obtained at  $-20$  °C from the concentrated *n* pentane solutions. Yield: 72 mg, 9%. Mp: 180.5–181.1 °C. Calcd for  $\text{C}_{29}\text{H}_{40}\text{CoN}_3\text{P}_2$  (551.54 g/mol): C, 63.15; H, 7.31; N, 7.62. Found: C, 62.89; H, 7.48; N, 7.74. IR (Nujol mull, KBr,  $\text{cm}^{-1}$ ): 1904  $\nu(\text{Co-H})$ , 944  $\rho(\text{PCH}_3)$ .  $^1\text{H}$  NMR (300 MHz,  $\text{C}_6\text{D}_6$ , 298 K, ppm):  $-21.21$  (t,  $J = 66$  Hz, 1H,  $\text{CoH}$ ), 0.65 (t',  $J = 6$  Hz, 18H,  $\text{PCH}_3$ ), 0.90 (t,  $J = 6$  Hz, 3H,  $\text{CH}_3$ ), 1.20 (m, 2H,  $\text{CH}_2$ ), 1.46 (m, 2H,  $\text{CH}_2$ ), 3.87 (t,  $J = 6$  Hz, 2H,  $\text{CH}_2$ ), 6.34 (d,  $J = 3$  Hz, 1H,  $H_{\text{arom}}$ ), 6.65 (t,  $J = 6$  Hz, 1H,  $H_{\text{arom}}$ ), 6.99–7.17 (m, 3H,  $H_{\text{arom}}$ ), 7.38–7.40 (d,  $J = 6$  Hz, 1H,  $H_{\text{arom}}$ ), 7.51–7.69 (m, 4H,  $H_{\text{arom}}$ ), 7.94–7.97 (d,  $J = 9$  Hz, 1H,  $H_{\text{arom}}$ ), 8.91–8.94 (d,  $J = 9$  Hz, 1H,  $H_{\text{arom}}$ ).  $^{31}\text{P}$  NMR (121 MHz,  $\text{C}_6\text{D}_6$ , 298 K, ppm): 17.18 (s,  $\text{PCH}_3$ ).  $^{13}\text{C}$  NMR (75 MHz,  $\text{C}_6\text{D}_6$ , 298 K, ppm): 12.5 ( $C_{\text{aliphatic}}$ ), 15.4 (t,  $^2J_{\text{P,C}} = 13.5$ ,  $\text{PCH}_3$ ), 18.8 ( $C_{\text{aliphatic}}$ ), 32.0 ( $C_{\text{aliphatic}}$ ), 48.9 ( $C_{\text{aliphatic}}$ ), 110.5 ( $C_{\text{aromatic}}$ ), 112.2 ( $C_{\text{aromatic}}$ ), 114.1 ( $C_{\text{aromatic}}$ ), 116.4 ( $C_{\text{aromatic}}$ ), 116.9 ( $C_{\text{aromatic}}$ ), 118.6 ( $C_{\text{aromatic}}$ ), 120.3 ( $C_{\text{aromatic}}$ ), 124.6 ( $C_{\text{aromatic}}$ ), 133.9 ( $C_{\text{aromatic}}$ ), 134.3 ( $C_{\text{aromatic}}$ ), 145.3 ( $C_{\text{aromatic}}$ ), 147.0 ( $C_{\text{aromatic}}$ ), 158.3 (NCN).

**4.6. Synthesis of 3b and 4b.** A 0.41 mL sample of *n* BuLi (2.5 M in hexane, 1.03 mmol) was added slowly to 30 mL of a THF solution of **2b** (400 mg, 0.94 mmol) at  $-78$  °C and the solution turned red. When the temperature returned to room temperature, the mixture was stirred for 30 min. After that, a solution of  $\text{CoMe}(\text{PMe}_3)_4$  (0.356 g, 0.94 mmol) in THF (30 mL) was added slowly to the resulting solution at  $-78$  °C. The reaction mixture was allowed to stir for 48 h at room temperature to provide a deep yellow solution. After the reaction, the solvents were removed under vacuum, and the residue was extracted with 100 mL of *n* pentane and 50 mL diethyl ether, respectively. The dark orange crystals of **4b** were obtained at  $-10$  °C from the concentrated diethyl ether solutions. Yield: 197 mg, 32%. Mp: 195.4–196.5 °C. Calcd for  $\text{C}_{40}\text{H}_{32}\text{CoN}_6$  (655.67 g/mol): C, 73.27; H, 4.92; N, 12.82. Found: C, 73.36; H, 5.06; N, 12.67. The light yellow crystals of **3b** were obtained at  $-20$  °C from the


concentrated *n* pentane solution. Yield: 67 mg, 14%. Mp: 172.0–172.5 °C. Calcd for  $\text{C}_{26}\text{H}_{34}\text{CoN}_3\text{P}_2$  (509.50 g/mol): C, 61.30; H, 6.73; N, 8.25. Found: C, 61.51; H, 6.79; N, 8.11. IR (Nujol mull, KBr,  $\text{cm}^{-1}$ ): 1920  $\nu(\text{Co-H})$ , 943  $\rho(\text{PCH}_3)$ .  $^1\text{H}$  NMR (300 MHz,  $\text{C}_6\text{D}_6$ , 298 K, ppm):  $-22.14$  (t,  $J = 69$  Hz, 1H,  $\text{CoH}$ ), 0.62 (t',  $J = 6$  Hz, 18H,  $\text{PCH}_3$ ), 3.16 (s, 3H,  $\text{CH}_3$ ), 6.20 (d,  $J = 3$  Hz, 1H,  $H_{\text{arom}}$ ), 6.61–6.66 (t,  $J = 6$  Hz, 1H,  $H_{\text{arom}}$ ), 7.02–7.05 (dd,  $J = 9$  Hz, 3 Hz, 1H,  $H_{\text{arom}}$ ), 7.09–7.15 (td,  $J = 6$  Hz, 3 Hz, 2H,  $H_{\text{arom}}$ ), 7.37–7.40 (d,  $J = 9$  Hz, 1H,  $H_{\text{arom}}$ ), 7.49–7.58 (m, 3H,  $H_{\text{arom}}$ ), 7.68–7.71 (m, 1H,  $H_{\text{arom}}$ ), 7.97–8.00 (d,  $J = 9$  Hz, 1H,  $H_{\text{arom}}$ ), 8.92–8.95 (dd,  $J = 9$  Hz, 1.1 Hz, 1H,  $H_{\text{arom}}$ ).  $^{31}\text{P}$  NMR (121 MHz,  $\text{C}_6\text{D}_6$ , 298 K, ppm): 17.82 (s,  $\text{PCH}_3$ ).  $^{13}\text{C}$  NMR (75 MHz,  $\text{C}_6\text{D}_6$ , 298 K, ppm): 15.5 (t,  $^2J_{\text{P,C}} = 12.75$ ,  $\text{PCH}_3$ ), 35.9 ( $C_{\text{aliphatic}}$ ), 110.1 ( $C_{\text{aliphatic}}$ ), 112.2 ( $C_{\text{aliphatic}}$ ), 113.9 ( $C_{\text{aliphatic}}$ ), 116.6 ( $C_{\text{aliphatic}}$ ), 116.9 ( $C_{\text{aliphatic}}$ ), 118.8 ( $C_{\text{aliphatic}}$ ), 119.5 ( $C_{\text{aliphatic}}$ ), 119.9 ( $C_{\text{aliphatic}}$ ), 124.3 ( $C_{\text{aliphatic}}$ ), 124.5 ( $C_{\text{aliphatic}}$ ), 124.6 ( $C_{\text{aliphatic}}$ ), 125.6 ( $C_{\text{aliphatic}}$ ), 133.9 ( $C_{\text{aliphatic}}$ ), 134.5 ( $C_{\text{aliphatic}}$ ), 145.0 ( $C_{\text{aliphatic}}$ ), 146.6 ( $C_{\text{aliphatic}}$ ), 158.4 (t,  $J = 1.7$  Hz, NCN).

**4.7. General Procedure for Cobalt-Catalyzed Hydrosilylation Reactions.** Under a  $\text{N}_2$  atmosphere, 1 mol % cobalt hydride **3** was added to a 20 mL Schlenk tube containing a magnetic stirrer without any solvent. Then, the alkene (1.00 mmol), *n* dodecane (170 mg, 1.00 mmol), pyridine *N* oxides (1 mol %, 0.9 mg, 0.01 mmol), and  $\text{Ph}_2\text{SiH}_2$  (1.2 equiv, 221 mg, 1.2 mmol) were added in order. The reaction mixture was stirred at room temperature for 24 h. The resulting solution was quenched with ethyl acetate. The combined organic fractions were concentrated in vacuum, and the crude product was purified by column chromatography on silica gel with petrol ether as eluent. The pure product was characterized by NMR analysis.

**4.8. X-ray Crystal Structure Determination.** Intensity data were collected on a Stoe Stadi Vari diffractometer with graphite monochromated  $\text{Ga K}\alpha$  radiation ( $\lambda = 0.71073$  Å). The structure was solved using the charge flipping algorithm, as implemented in the program SUPERFLIP,<sup>32</sup> and refined by full matrix least squares techniques against  $F^2$  (SHELXL)<sup>33</sup> through the OLEX interface.<sup>34</sup> All non hydrogen atoms were refined anisotropically, and all hydrogen atoms except for those of the disordered solvent molecules were placed using AFIX instructions. Appropriate restraints or constraints were applied to the geometry and the atomic displacement parameters of the atoms. 1876054 (**3b**), 1883487 (**4a**), and 1894294 (**4b**) contain the supplementary crystallographic data for this paper.

## ■ AUTHOR INFORMATION

### Corresponding Authors

Hongjian Sun – School of Chemistry and Chemical Engineering, Key Laboratory of Special Functional Aggregated Materials, Ministry of Education, Shandong University, Jinan, Shandong 250100, People's Republic of China;  [orcid.org/0000-0003-1237-3771](https://orcid.org/0000-0003-1237-3771); Email: [hjsun@sdu.edu.cn](mailto:hjsun@sdu.edu.cn)

Xiaoyan Li – School of Chemistry and Chemical Engineering, Key Laboratory of Special Functional Aggregated Materials, Ministry of Education, Shandong University, Jinan, Shandong

## Authors

**Shangqing Xie** – School of Chemistry and Chemical Engineering, Key Laboratory of Special Functional Aggregated Materials, Ministry of Education, Shandong University, Jinan, Shandong 250100, People's Republic of China

**Olaf Fuhr** – Institut für Nanotechnologie (INT) und Karlsruher Nano Micro Facility (KNMF), Karlsruher Institut für Technologie (KIT), Eggenstein Leopoldshafen 76344, Germany

**Dieter Fenske** – Institut für Nanotechnologie (INT) und Karlsruher Nano Micro Facility (KNMF), Karlsruher Institut für Technologie (KIT), Eggenstein Leopoldshafen 76344, Germany

## Notes

The authors declare no competing financial interest.

## ACKNOWLEDGMENTS

This work was supported by NSF China 21572119/21971151 and NSF Shandong ZR2019ZD46.

## REFERENCES

- (1) (a) Marciniak, B. Catalysis by transition metal complexes of alkene silylation—recent progress and mechanistic implications. *Coord. Chem. Rev.* **2005**, *249*, 2374–2390. (b) Nakajima, Y.; Shimada, S. Hydrosilylation reactions of olefins: recent advances and perspectives. *RSC Adv.* **2015**, *5*, 20603–20616. (c) Obligation, J. V.; Chirik, P. J. Earth abundant transition metal catalysts for alkene hydrosilylation and hydroboration. *Nat. Rev. Chem.* **2018**, *2*, 15–34.
- (2) Herzig, C. *Siloxane copolymers containing alkenyl groups*. US 6265497B1, 2001.
- (3) Lewis, L. N.; Stein, J.; Gao, Y.; Colborn, R. E.; Hutchins, G. Platinum catalysts used in the silicones industry. *Platinum Met. Rev.* **1997**, *41*, 66–75.
- (4) Chalk, A. J.; Harrod, J. F. Reactions between Dicobalt Octacarbonyl and Silicon Hydrides. *J. Am. Chem. Soc.* **1965**, *87*, 1133–1135.
- (5) Brookhart, M.; Grant, B. E. Mechanism of a cobalt(III) catalyzed olefin hydrosilylation reaction: direct evidence for a silyl migration pathway. *J. Am. Chem. Soc.* **1993**, *115*, 2151–2156.
- (6) Du, X.; Zhang, Y.; Peng, D.; Huang, Z. Base Metal Catalyzed Regiodivergent Alkene Hydrosilylations. *Angew. Chem., Int. Ed.* **2016**, *55*, 6671–6675.
- (7) (a) Gao, Y.; Wang, L.; Deng, L. Distinct Catalytic Performance of Cobalt(I)–N Heterocyclic Carbene Complexes in Promoting the Reaction of Alkene with Diphenylsilane: Selective 2,1 Hydrosilylation, 1,2 Hydrosilylation, and Hydrogenation of Alkene. *ACS Catal.* **2018**, *8*, 9637–9646. (b) Cheng, Z.; Xing, S.; Guo, J.; Cheng, B.; Hu, L.; Zhang, X.; Lu, Z. Highly Regioselective Sequential 1,1 Dihydrosilylation of Terminal Aliphatic Alkynes with Primary Silanes. *Chin. J. Chem.* **2019**, *37*, 457–461. (c) Guo, J.; Wang, H.; Xing, S.; Hong, X.; Lu, Z. Cobalt Catalyzed Asymmetric Synthesis of gem Bis(silyl) alkanes by Double Hydrosilylation of Aliphatic Terminal Alkynes. *Chem.* **2019**, *5*, 881–895.
- (8) (a) Liu, Y.; Deng, L. Mode of Activation of Cobalt(II) Amides for Catalytic Hydrosilylation of Alkenes with Tertiary Silanes. *J. Am. Chem. Soc.* **2017**, *139*, 1798–1801. (b) Raya, B.; Jing, S.; Balasanthiran, V.; RajanBabu, T. V. Control of Selectivity through Synergy between Catalysts, Silanes, and Reaction Conditions in Cobalt Catalyzed Hydrosilylation of Dienes and Terminal Alkenes. *ACS Catal.* **2017**, *7*, 2275–2283.

(9) Mo, Z.; Liu, Y.; Deng, L. Anchoring of Silyl Donors on a Nheterocyclic Carbene through the Cobalt Mediated Silylation of Benzylic C H Bonds. *Angew. Chem., Int. Ed.* **2013**, *52*, 10845–10849.

(10) Wang, C.; Teo, W. J.; Ge, S. Cobalt Catalyzed Regiodivergent Hydrosilylation of Vinylarenes and Aliphatic Alkenes: Ligand and Silane Dependent Regioselectivities. *ACS Catal.* **2017**, *7*, 855–863.

(11) Lee, K. L. (Aminomethyl)pyridine Complexes for the Cobalt Catalyzed Anti Markovnikov Hydrosilylation of Alkoxy or Siloxy (vinyl)silanes with Alkoxy or Siloxyhydrosilanes. *Angew. Chem., Int. Ed.* **2017**, *56*, 3665–3669.

(12) Sang, H.; Yu, S.; Ge, S. Cobalt Catalyzed Regioselective Stereoconvergent Markovnikov 1,2 Hydrosilylation of Conjugated Dienes. *Chem. Sci.* **2018**, *9*, 973–978.

(13) Chen, C.; Hecht, M. B.; Kavara, A.; Brennessel, W. W.; Mercado, B. Q.; Weix, D. J.; Holland, P. L. Rapid, Regioconvergent, Solvent Free Alkene Hydrosilylation with a Cobalt Catalyst. *J. Am. Chem. Soc.* **2015**, *137*, 13244–13247.

(14) (a) Cheng, B.; Lu, P.; Zhang, H.; Cheng, X.; Lu, Z. Highly Enantioselective Cobalt Catalyzed Hydrosilylation of Alkenes. *J. Am. Chem. Soc.* **2017**, *139*, 9439–9442. (b) Chen, J.; Guo, J.; Lu, Z. Recent Advances in Hydrometallation of Alkenes and Alkynes via the First Row Transition Metal Catalysis. *Chin. J. Chem.* **2018**, *36*, 1075–1109. (c) Chen, J.; Lu, Z. Asymmetric Hydrofunctionalization of Minimally Functionalized Alkenes via Earth Abundant Transition Metal Catalysis. *Org. Chem. Front.* **2018**, *5*, 260–272. (d) Zaranek, M.; Pawluc, P. Markovnikov Hydrosilylation of Alkenes: How an Oddity Becomes the Goal. *ACS Catal.* **2018**, *8*, 9865–9876.

(15) Pappas, I.; Treacy, S.; Chirik, P. J. Alkene Hydrosilylation Using Tertiary Silanes with  $\alpha$  Diimine Nickel Catalysts. Redox Active Ligands Promote a Distinct Mechanistic Pathway from Platinum Catalysts. *ACS Catal.* **2016**, *6*, 4105–4109.

(16) Sun, Y.; Li, X.; Sun, H. [CNN] pincer nickel(II) complexes of N heterocyclic carbene (NHC): synthesis and catalysis of the Kumada reaction of unactivated C–Cl bonds. *Dalton Trans.* **2014**, *43*, 9410–9413.

(17) Lubitz, K.; Radius, U. The Coupling of N Heterocyclic Carbenes to Terminal Alkynes at Half Sandwich Cobalt NHC Complexes. *Organometallics* **2019**, *38*, 2558–2572.

(18) Bhattacharjee, A.; Chavarot Kerlidou, M.; Andreiadis, E. S.; Fontecave, M.; Field, M. J.; Artero, V. Combined Experimental–Theoretical Characterization of the Hydrido Cobaloxime [HCo(dmgH)<sub>2</sub>(PnBu<sub>3</sub>)]. *Inorg. Chem.* **2012**, *51*, 7087–7093.

(19) Liang, Q.; Janes, T.; Gjergji, X.; Song, D. Iron complexes of a bidentate picolyl NHC ligand: synthesis, structure and reactivity. *Dalton Trans.* **2016**, *45*, 13872–13880.

(20) Liang, Q.; Liu, N. J.; Song, D. Constructing reactive Fe and Co complexes from isolated picolyl functionalized N heterocyclic carbenes. *Dalton Trans.* **2018**, *47*, 9889–9896.

(21) Tamotsu, T. *Preparation of organosilicon compounds*. JP 2001328990A, 2001.

(22) Lam, Y. C.; Nielsen, R. J.; Goddard, W. A., III; Dash, A. K. The mechanism for catalytic hydrosilylation by bis(imino)pyridine iron olefin complexes supported by broken symmetry density functional theory. *Dalton Trans.* **2017**, *46*, 12507–12515.

(23) Mathew, J.; Nakajima, Y.; Choe, Y. K.; Urabe, Y.; Ando, W.; Sato, K.; Shimada, S. Olefin hydrosilylation catalyzed by cationic nickel(II) allyl complexes: a non innocent allyl ligand assisted mechanism. *Chem. Commun.* **2016**, *52*, 6723–6726.

(24) (a) Wang, C.; Teo, W. J.; Ge, S. Cobalt Catalyzed Regiodivergent Hydrosilylation of Vinylarenes and Aliphatic Alkenes: Ligand and Silane Dependent Regioselectivities. *ACS Catal.* **2017**, *7*, 855–863. (b) Cheng, B.; Liu, W.; Lu, Z. Iron Catalyzed Highly Enantioselective Hydrosilylation of Unactivated Terminal Alkenes. *J. Am. Chem. Soc.* **2018**, *140*, 5014–5017.

(25) Chalk, A. J.; Harrod, J. F. Homogeneous Catalysis. II. The Mechanism of the Hydrosilylation of Olefins Catalyzed by Group VIII Metal Complexes. *J. Am. Chem. Soc.* **1965**, *87*, 16–21.

(26) Klein, H. F.; Hammer, R.; Gross, J.; Schubert, U. Olefin Insertion into Cobalt(d<sup>8</sup>) Complexes Structure of Ethylene(phenyl)



tris(trimethylphosphane)cobalt. *Angew. Chem., Int. Ed. Engl.* **1980**, *19*, 809–810.

(27) Mukhopadhyay, T. K.; Flores, M.; Groy, T. L.; Trovitch, R. J. A  $\beta$  diketiminate manganese catalyst for alkene hydrosilylation: substrate scope, silicone preparation, and mechanistic insight. *Chem. Sci.* **2018**, *9*, 7673–7680.

(28) Tokmic, K.; Markus, C. R.; Zhu, L.; Fout, A. R. Well Defined Cobalt(I) Dihydrogen Catalyst: Experimental Evidence for a Co(I)/Co(III) Redox Process in Olefin Hydrogenation. *J. Am. Chem. Soc.* **2016**, *138*, 11907–11913.

(29) Gribble, M. W.; Pimot, J. M. T.; Bandar, J. S.; Liu, R. Y.; Buchwald, S. L. Asymmetric Copper Hydride Catalyzed Markovnikov Hydrosilylation of Vinylarenes and Vinyl Heterocycles. *J. Am. Chem. Soc.* **2017**, *139*, 2192–2195.

(30) Hu, M.; He, Q.; Fan, S.; Wang, Z.; Liu, Y.; Mu, Y.; Peng, Q.; Zhu, S. Ligands with 1,10 phenanthroline scaffold for highly regioselective iron catalyzed alkene hydrosilylation. *Nat. Commun.* **2018**, *9*, 221.

(31) Klein, H. F.; Karsch, H. H. Methyltetrakis (trimethylphosphin)kobalt und seine Derivate. *Chem. Chem. Ber.* **1975**, *108*, 944–955.

(32) Palatinus, L.; Chapuis, G. SUPERFLIP. A Computer Program for the Solution of Crystal Structures by Charge Flipping in Arbitrary Dimensions. *J. Appl. Crystallogr.* **2007**, *40*, 786–790.

(33) Sheldrick, G. M. A Short History of SHELX. *Acta Crystallogr., Sect. A: Found. Crystallogr.* **2008**, *A64*, 112–122.

(34) Dolomanov, O. V.; Bourhis, L. J.; Gildea, R. J.; Howard, J. A. K.; Puschmann, H. OLEX2: A Complete Structure Solution, Refinement and Analysis Program. *J. Appl. Crystallogr.* **2009**, *42*, 339–341.